



HAL
open science

Pigments and glassy matrix of the 17th -18th century enamelled French watches: A non-invasive onsite Raman and pXRF study

Philippe Colomban, Burcu Kirmizi, Catherine Gougeon, Michele Gironda,
Catherine Cardinal

► To cite this version:

Philippe Colomban, Burcu Kirmizi, Catherine Gougeon, Michele Gironda, Catherine Cardinal. Pigments and glassy matrix of the 17th -18th century enamelled French watches: A non-invasive onsite Raman and pXRF study. *Journal of Cultural Heritage*, 2020, 44, pp.1-14. 10.1016/j.culher.2020.02.001 . hal-03373805

HAL Id: hal-03373805

<https://hal.science/hal-03373805>

Submitted on 11 Oct 2021

HAL is a multi-disciplinary open access archive for the deposit and dissemination of scientific research documents, whether they are published or not. The documents may come from teaching and research institutions in France or abroad, or from public or private research centers.

L'archive ouverte pluridisciplinaire **HAL**, est destinée au dépôt et à la diffusion de documents scientifiques de niveau recherche, publiés ou non, émanant des établissements d'enseignement et de recherche français ou étrangers, des laboratoires publics ou privés.

1. Research aims

Enamel refers to any kind of glassy coatings that can be fused on a variety of substrates such as metal, glass and ceramics with firing in the form of coloured and/or opacified glass. The typical composition of an enamel includes glassy aluminosilicates and colouring/opacifying agents which are mainly the pigments because the small thickness of the coating imposes a high power of colouration. The flux content (soda, potash, borax, fluorite, bismuth) determines the firing temperature and viscosity. Enamelling may be considered as the most sophisticated branch of the arts of fire which eventually evolved with mastering of fire by mankind preceding the Antiquity. Fixed by the firing process, the enamelled decor is resistant to keep its glossy surface without any additional protective layer, which allows daily use of enamelled objects. The earliest uses of coloured enamel are observed in objects dating as early as the 15th century B.C. both in the Mediterranean/Eastern civilizations (Egypt, Cyprus and Mesopotamia) and China on pottery, glass and metal substrates [1-3]. Enamelling techniques developed during the Celtic, Roman and Byzantine periods particularly with the production of sophisticated metal wares such as jewellery and reliquaries along with glass and pottery [2,4-6]. The *cloisonné* technique is one of the finest types of enamelling practices on metal, as mastered by the Celtic and then Byzantine craftsmen mainly from the 8th century onwards [2,4-7]. This technique is considered to have been transferred to China via the Silk Road [7,8], making a big influence on the Far Eastern production of enamelled objects on metal. In the meantime, Normand and Islamic and glassmakers and potters reached a very high level in the craft of glass and pottery enamelling from the 12th century onwards [9-14]. Then, northern Italy became a centre in the production of enamelled glass by the 15th century, in relation to a well-established glass industry, namely in Venice and Altare [15-17] and enamelled pottery (majolica) in many towns [3,18]. Metal wares with painted enamels were also being produced during the 15th century in Italy as well as in the Netherlands [2,19,20] but the real development of the painted enamelling technique on metal occurred in Limoges in the southwest of France during the 16th century [2,19-24]. Fused onto various types of utensils made of copper alloys, painted enamels of Limoges represent the technical supremacy of the French Renaissance with multi-coloured enamelled decorations of elaborate scenes and figures on the entire metal surface with a sophisticated know-how of the use of different enamel compositions and subsequent firing cycles [2,7,20-24]. Following this, the first half of the 17th century witnessed the emergence of a new craft, namely the enamel portrait miniatures which were introduced to France by goldsmiths as Jean and Henri Toutin, based on the miniaturisation of painted enamels on the gold substrate [25-27]. All productions of these painted enamels on various types and forms of metal substrates displaying pictorial decorations had generated an artistic manner which was similar to painting, such as oil easel painting on wood, canvas or copper plate and also

tempera miniatures on ivory, copper and paper. However, the superiority of a painted enamel decoration comes from its relatively permanent lifetime, without any fading and darkening. Analyses of ancient recipes point out that the painting technique of Limoges and miniature enamels were different [27-30]. Regarding the application of the enamels, enamel powders had been painted with water medium, also sometimes with the addition of proteic glue, on copper alloys at Limoges workshops although turpentine or lavender essences (*huiles grasses*: fatty oils prepared by exposition of essence to air) had been used for enamel painting on gold. In both cases, multi-firings between ca. 600°C and 800°C had been performed to obtain the desired final hues. Information on the ingredients lists the use of tin oxide for white, *safran de Mars* (i.e. synthetic iron oxides) for yellow to red, lapis lazuli and/or *saffre* (smalt) for blue as well as tin, lead and nitre ores for yellow. Copper was reputed to be not sufficient to get a 'nice' green and mixing of blue and yellow materials were recommended [28-30].

First watches appeared at the very end of the 15th century as very prestigious objects with the miniaturisation of clock movement [25-27]. Indeed, the craft of mechanics first developed in the second half of the 17th century and the beginning of the 18th century in England and in France with the necessity to measure the time accurately, as required for the measurement of longitude on ships. Worn at the waist or neck, integrated with jewels or canes, the decorative potential of these miniaturised clocks caught the attention of goldsmiths who adorned them with stones and pearls, painted enamels and engravings. The emergence of watches with painted enamel miniatures as a new form of fine art occurred circa 1630 in France [25]. Designed also to be real fashion accessories, watches with gold case could be worn on the belt and after many decades on the back of the gusset (pocket). Decorations of these watches represent the highest level of the enamelling technology achieved, allowing the reproduction of the works of famous painters, often popularized by the edition of prints [25]. At the same time, the painters were closely following the evolution of artistic styles and trends. The name of the movement maker was often engraved in the metal and rarely, the signature of the painter/enameller was painted in a corner or inside (recto and verso of the lid and the bottom of the box are generally decorated).

In this study, we present the first analytical study of twelve rare enamelled watches, mostly produced in France and selected from the collection of Musée du Louvre [26]. Due to the high value of the objects, the use of non-invasive mobile techniques such as Raman microspectroscopy and X-ray fluorescence was essential. This study is part of the research program conducted on the 17th century European enamelled objects (metal ware, glass and pottery) in order to compare the European technology with that used in similar Chinese productions from the end of Kangxi reign (1662–1722) and during the Yongzheng (1723–1735) reign [7,31-36]. In fact, historical records attest that enamelled objects including clocks and watches were given as presents to the Chinese Court by

the Jesuits and ambassadors of Louis XIV, the Sun King and it is considered that sophisticated painted decorations of these items were envied by the Kangxi Emperor who developed a strong interest to have the similar type of painted enamel productions in China [31,32]. The present research program has the objective to define the non-invasive mobile scientific procedure for the analysis of these masterpieces in order to identify the enamelling technology used and therefore characterize the artefacts made in China with imported raw materials and/or technology.

Previous studies have demonstrated that Raman microspectroscopy is an efficient non-invasive technique for the materials characterization of old artefacts such as glass, enamels on metal and glazed pottery which are highly prized and cannot be transferred from the museums to the laboratory [37-40]. For the recent years, portable XRF systems have also been increasingly used for the non-invasive elemental analysis of glassy artefacts which have an art-historical value [38-40]. These particular techniques have also been used for the study of enamelled objects, with metal or ceramic bases [7,8,21].

Comprehensive studies of Limoges enamels [7,20-24] have previously pointed out the variation of the enamel compositions, in particular the increase of the PbO content from the 16th to the 19th century with the shift from mixed potash-soda to potash-lead flux which were both identified by Raman spectroscopy and XRF. Previous studies of Limoges [7,20-24], Chinese [8,41,42] and Japanese [43-45] enamels showed that different technologies for the achievement of different colours such as blue, yellow, green, white and red could be identified by Raman scattering and XRF elemental analyses. This preliminary on-site study will thus focus on the characterization of the enamels with the above-mentioned colours including the identification of phases, chromophores, major and minor elements. The number of studied objects is limited but the selected painted enamelled watches cover the period from the beginning (ca. 1630) of the production to the first half of the 18th century in order to get a first representative view of the evolution of the painting/enamelling technique on gold.

Furthermore, analytical studies of jewellery, especially the ones with non-invasive on-site procedures are very limited and rather focused on the identification of 'gems' or their replacement by synthetic glass [46-54]. As a rare example, the enamelled jewellery of René Lalique from the 20th century (Art Déco style) has recently been analysed by the combination of Raman spectroscopy and XRF which were although carried out at the laboratory [55].

2. Experimental

2.1 Artefacts

The watches analysed are listed in Table 1 and shown in Figures 1 to 3. They belong to the collections of Musée du Louvre in Paris and most of them are exhibited in the showcases of the museum. All the watches are described in the museum catalogue [26]. Table 1 includes the name of the painter/enameller when the signature is present on the artefact. In the case of the absence of signature, potential attribution made by comparison with similar documented artefacts is indicated with a question mark. The movement maker is also indicated when the signature is present. Analysed spots are visible on the figures given as Supplementary Materials. The subject of the enamelled decor is identified [26,56] by comparison with the paintings and/or prints of the same period. Most of these watches are from workshops located in Paris while some of them are from Blois which was still an important production centre during the 17th century. It should be noted that the itinerancy of the French Court between Paris and Loire Castle Valley only really stopped at the end of the 16th century [57] and Paris workshops then replaced those of Blois. Watches produced in London, Basel and Amsterdam, were also selected for the present study. Indeed, the development of watchmaking, which was initiated in northern Italy and at the Burgundy Court, then spread out in France and Europe with the displacement of many Huguenots abroad, including in Swiss (Geneva) [58].

Table 1: Studied artefacts: historical information and places of production (after [26]); artefacts also analysed by pXRF are noted.

Inventory number	Thickness & Diameter (cm)	Subject	Painter / Enameller	Movement maker	Place	Date	pXRF
OA8429	1.6; 5	<i>Perseus delivering Andromeda</i>		Robert Chevallier	Blois	circa 1630-1640	
OA8428	1.8; 5.8	<i>The Virgin and the child</i>		Josias Jolly	Paris	circa 1640	
OA7074	2; ~5	<i>Vision of Saint-Hubert</i>		Jehan Augier	Paris	circa 1640	X
OA8318	3; 6.8	<i>The boarding of Chariclea</i>		G. Gamot	Paris	mid 17 th c.	
OA10077	2; ~5	<i>Battle of Emperor Constantine</i>	Robert Vauquer (assignment)		Blois	mid 17 th c.	X
OA7075	2; ~5	<i>Ceres, Bacchus, Venus and Love</i>	Jean II Toutin		Chateaudun (?)	mid 17 th c.	
OA8435	2.1; 3.8	<i>Aurora and Cephalus</i>	Jean-Pierre & Amy Huaud		France	circa 1700	X
OA8432	2.5; 4.6	<i>The farewells of Dido and Aeneas</i>		Roger Dunster	London	Last quarter of 17 th c.	
OA10079	2.1; ~4.5	<i>Bouquet of flowers</i>	F. Braun	Enderlin	Bale (Swiss)	End 17 th c./ beginning of 18 th c.	X
OA6224	2.5; ~4.5	<i>Meleager and Diane</i>		William Koster	Amsterdam (Low Countries)	2 nd quarter of 18 th c.	X
OA8338	2.3; 4.4	<i>Hercules and Omphale</i>	Decombaz	Jean-Baptiste Baillon	Paris	2 nd quarter of 18 th c.	
OA8337	2.4; 4.5	<i>Hercules and Omphale</i>		Julien Le Roy	Paris	1732-1738 mark	

2.2 Raman microspectroscopy

Non-invasive Raman analyses were performed at the collections of Musée du Louvre (Paris) with a mobile HORIBA Scientific Jobin-Yvon (France) Raman set-up. In this set-up, optic fibres are used to connect the HE532 spectrometer (920 lines/mm; resolution $\sim 4 \text{ cm}^{-1}$) to a remote SuperHead® and 532 nm Ventus Quantum 300 mW laser. The SuperHead® was placed on a heavy and very stable stage with XYZ micrometric displacements in order to record the Raman spectra of the samples in stable conditions. The Horiba Scientific CCD is cooled at 200 K. A reliable spectrum starts over 80 cm^{-1} but a flat background is only achieved over 500 cm^{-1} . Due to the light absorption by the colour of the analysed matter, the shape of the background is variable: flat for a blue area, decreasing for a red area and increasing for yellow and green areas.

A x50 Nikon ($\sim 17 \text{ mm}$ long working distance) microscope objective was used for the analysis of the enamelled watches which were suspended from a hook embedded in a stable wooden support. The probed volume was about $4 \times 4 \times 15 \text{ }\mu\text{m}^3$ for the poor absorbing colours. Definition of the exact probed volume is difficult because Airy formula does not make sense when the adjacent phases may display a Raman signal which differs 5, 10 or even 100 times. For dark colours, the absorption strongly limits the penetration of the laser light to a few microns or less depth. The power of illumination at the SuperHead was controlled roughly with a variable shutter. The focus quality was checked by visual examination at very low laser power in the dark. The sample and SuperHead were covered with a black textile in order to prevent the contribution from the ambient light and protect the operator's eyes from the laser scattering. The focus was first adjusted with the XYZ micrometre stage up to have the maximum level of counts on the laptop screen which corresponds to a focus at the sample surface. During the measurements, the laser power was switched from about 1 mW (black and dark colours) to 10 mW (white and yellow areas) according to the colour of the analysed areas of the samples. Good spectra were recorded from the very surface to the sub layers by modifying the focus. At least three spots were analysed for each coloured area. Recording times of the spectra range between a few seconds and a few minutes as a function of the number of accumulations required (3 to 100). Changing the focus from the enamel surface towards the metal substrate allowed us to estimate the enamel thickness as hundred(s) of microns.

2.3. X-ray Fluorescence

Portable XRF (pXRF) measurements were collected using an Elio instrument (ELIO, XGLab Bruker, Italy) which consists of a miniature X-ray tube system with a Rh anode (max voltage of 50 kV, max current of 0.2 mA, and a 1 mm collimator) and a large area Silicon Drift Detector (SDD) (50 mm² active area) with energy resolution of $< 140 \text{ eV}$ for Mn K_α, an energy range of detection from 1 keV to

40 keV, and a maximum count rate of 5.6×10^5 cps. Measurements were made in the point mode, using a tube voltage of 40 kV and current of 100 μ A and acquisition time of 40 s. No filter was applied between the X-ray tube and the sample. Working distance (distance between the sample and the detector) during analysis was around 15 mm with the distance between the instrument front and the artefact about 10 mm. The set-up parameters used were selected to provide high spectral signal while optimizing the signal to noise ratio (SNR). Information thickness during the analysis of the enamel is estimated to be $\sim 4 \mu\text{m}$ at Si K_{α} , 130 μm at Cu K_{α} , 220 μm at Au L_{α} and 2.5 mm at Sn K_{α} . Measurement data were processed using the data reduction software provided by the factory, which enables automatic peak recognition supported by manual peak selection and checking. The software further enables curve fitting based on chosen elements to ensure a match between the measured spectra and theoretically predicted spectra calculated from fundamental parameters (FP). Where the sample thickness satisfies infinite thickness criteria for the elements of interest, semi-quantitative compositions were also calculated using FP by the instrument software.

3. Results

3.1 Colouring agents

3.1.1 Raman microspectroscopy

All spectra recorded on the 17th-18th century enamelled watches are presented in Supplementary Material. Figures 4 and 6 show the representative spectra displaying various Raman signatures. Figures 5 and 7 compare the representative spectra recorded for yellow and blue areas as the coloured areas in which the variation of the signature appears to be maximal. Table 2 lists the phases identified together with the comparative data of enamelled artefacts previously studied and reference works [16,21,33-35,59-77].

Pigments identified are similar to those commonly observed for Limoges enamels, such as cassiterite (SnO_2 , lead arsenate apatite) for white, hematite ($\text{Fe}_{2-x}\text{M}_x\text{O}_3$, $\text{M} = \text{Ti, Al}$) for red hues and *Naples Yellow* type ($\text{Pb}_{2-x}\text{M}'_x\text{M}_2\text{-yM}''_y\text{O}_{7-\delta}$) for yellow and green (mixed with blue matrix for the latter). Blue areas show the characteristic signature of cassiterite but some artefacts show additional features, such as the more or less strong peak at $\sim 820 \text{ cm}^{-1}$, characteristic of the As-O stretching mode of lead arsenates [7,33,34,75-77]. The strongest peak was detected in the blue area of OA8435 (Figure 4) while less strong peaks were encountered in OA8338 and OA8318 (Figure 6). The narrow $\sim 820 \text{ cm}^{-1}$ peak with a well-defined shoulder at $\sim 780 \text{ cm}^{-1}$ is an indicator of the lead arsenate apatite phase $\text{Na}_{1-x-y}\text{K}_x\text{Ca}_y\text{Pb}_4(\text{AsO}_4)_3$ [16,34,75,76] which is formed by cooling on the reaction of cobalt ores containing arsenic (CoAs_2 , CoAs_3 , CoAsS , etc.), from European mines with lead-based enamel. The broadness

and position of the peak vary consistently with the parent arsenate phases, as identified by SEM-EDX and microdiffraction in some ancient enamelled (glazed) artefacts [16] and distinguishing the different phases from their sole Raman signature requires further studies.

Carbon, Fe-based spinel and manganese oxide were detected in the black and shaded (dark) areas. Manganese oxide was particularly detected in the black area of OA10077 with a strong broad peak at $\sim 580 \text{ cm}^{-1}$ and likely in the orange area of OA8432 with a broad peak at $\sim 630 \text{ cm}^{-1}$ [64] (see Supplementary Material). The characteristic peaks of lazurite chromophore (S_3^- ion) with the main peak at 542 cm^{-1} stretching mode [61,70] were detected in one of the samples (OA8338) in the body skin (Figure 6). Lazurite mineral is the main constituent of lapis lazuli which is actually a type of metamorphic rock, commonly used as a natural source of blue pigment for blue decoration in glass in the past [9,10]. Due to the resonance effect of S_3^- chromophore under green laser excitation [70], the amount of the blue chromophore can be very small and may also result from the contamination of the pencil probably used for painting or a restoration practice. Another unexpected feature is the strong broad peak at $\sim 310 \text{ cm}^{-1}$ observed in the green area of OA8318, pointing to the presence of amorphous arsenic sulphide (Figure 6). The possible presence of this yellow compound that was mixed with the blue pigment to give the green colour, may correspond to a restoration practice in the past since its thermal stability is *a priori* too low to be stable at the firing temperature of the enamel (typically from $\sim 500^\circ\text{C}$ to 800°C).

Some red to purple/violet areas display Raman spectra without any strong peaks, but with a characteristic 'fluorescence' spectrum (maximal at $\sim 500\text{-}600 \text{ cm}^{-1}$, actually ca. 550 nm in the absolute scale should be used for fluorescence). This shape is characteristic of the combined contribution of fluorescence and absorption when gold (Au^0) nanoparticles are dispersed in the glassy silicate matrix of the enamel. This method was initiated by the famous glassmaker Bernard Perrot at Orléans after mid-17th century [15,16,78] and then used by Johann Kunckel in Germany [78,79], the colour also being called Cassius' purple when used on ceramics [33,60]. Small bands can be detected in some cases, corresponding to those of cassiterite ($\sim 631\text{-}771 \text{ cm}^{-1}$ doublet), for instance in OA8338 (Figure 6) and the glassy matrix (broad feature at $\sim 1000 \text{ cm}^{-1}$, Figure 7). However, traces of calcium antimonate type opacifiers such as $\text{Ca}_2\text{Sb}_2\text{O}_7$ ($\sim 480\text{-}633 \text{ cm}^{-1}$ doublet) and CaSb_2O_6 (671 cm^{-1}) [64] cannot be excluded due to the presence of small peaks at the characteristic wavenumbers. The main peak of calcium antimonate overlaps with that of the ambient bulb light (479 cm^{-1} , Figure 4- bottom) which cannot be always totally wiped off with the (nearly opaque) black textile covering the sample and the remote head.

All the yellow areas of the 17th-18th century enamelled watches display the characteristic Raman signature of *Naples yellow* type pigment which is in fact a generic name comprising modified forms

of the lead pyrochlore compound. As well documented by the literature [62-69,71-74], the chemical nature of lead pyrochlore solid solution ($\text{Pb}_{2-x}\text{M}'_x\text{M}_{2-y}\text{M}''_y\text{O}_{7-\delta}$) leads to much variable compositions ($\text{M}, \text{M}'' = \text{Sb}, \text{Sn}, \text{Fe}, \text{Si}, \text{Zn}$; $\text{M}' = \text{RE}$), forming the so-called 'defect' pyrochlores. Some elements with different speciation (e.g. Sn^{2+} or Sn^{4+} , Sb^{3+} or Sb^{5+} , Fe^{2+} or Fe^{3+}), the oxygen non-stoichiometry in these compounds depend on variable conditions of the firing atmosphere, either reducing or oxidizing. The use of end-members of lead pyrochlore solid solutions including almost only Sn (Pb_2SnO_4 also called Type I, Type II being partially substituted with silicon) and only Sb ($\text{Pb}_2\text{Sb}_2\text{O}_7$, mineral pigment called bindheimite) have also been documented. All of these compositional variations are reflected in the Raman signature of *Naples yellow* type pigment with some modifications in the characteristic signature. Sb-rich *Naples Yellow* shows strong peaks at ~ 110 - 120 (Pb^{2+} translational mode) and $\sim 505 \text{ cm}^{-1}$ (the mode involving Sb-O stretching vibration). Alternatively, Sn-rich compositions exhibit stronger peaks at ~ 130 , 335 and 450 cm^{-1} (the latter mode involves Sn-O stretching component) with the disappearance of the $\sim 505 \text{ cm}^{-1}$ peak [16,21,66]. However, firing conditions such as temperature and atmosphere may also shift the wavenumber of the above characteristic bands. Raman spectra obtained from the yellow areas of the samples analysed display bands similar to those corresponding to Sb-rich and Sn-rich *Naples yellow* type pigment (Figures 4, 6). Variation of the Raman signature in these samples is in good correlation with variable compositions detected by pXRF (Table 3). A third type of Raman spectrum is characterized by strong peaks at ~ 130 and $\sim 335 \text{ cm}^{-1}$ with a triplet of medium intensity peaks at ~ 450 - 480 and 505 cm^{-1} (Figures 4, 6). This signature is assigned to the presence of a more complex solid solution (see 3.1.2).

An important point to be noted is the observation of the Raman signature of different colouring phases at different intensities in almost all the analysed spots, from very low to very strong. For instance, peaks corresponding to cassiterite and *Naples Yellow* type pigment with variable intensities were detected in some of the spectra recorded in the red area of OA8435 (Figure 4), the white areas of OA6224 and OA8338 (Figures 4, 6) as well as in the blue area of OA8318 (Figure 6). Another example is the coexistence of lapis lazuli and *Naples Yellow* in the skin area of OA8338 (Figure 6). This is very different from the Raman spectra recorded on Limoges enamels which most frequently show 'pure' signature of the glassy matrix and/or 'simple' superimposition of only one pigment [7,21].

Table 2: Identified pigments with the principal characteristic Raman peaks.

Inventory number	Date	Phases (peak/cm ⁻¹)	Colour	Remarks
OA8429	circa 1630-1640	Cassiterite (631) Naples yellow (130,335,450,505) Hematite (1310,218,287) Carbon (1350,1565)	white,blue yellow,green red dark blue and red shade	
OA8428	circa 1640	Cassiterite (631) Naples yellow (130,335,450,505) Hematite (1310,218,280) Carbon (1570)	white,blue yellow red violet, black	Blue: 820 cm ⁻¹ shoulder
OA7074	circa 1640	Cassiterite (631) Naples Yellow (132,335,450,505) Hematite (1315,220,278)	white,blue yellow,green red	
OA8318	mid 17 th c.	Cassiterite (631) Naples Yellow (132,335,450,505) Hematite (1313,220,288) Arsenic sulphide (311?)	blue yellow, green brown green	Blue: 820 cm ⁻¹ shoulder
OA10077	mid 17 th c.	Cassiterite (631) Naples Yellow (132,336,450-480-502) Carbon (1335,1555) Mn-oxide (580)	white,green,blue yellow,green black black	
OA7075	mid 17 th c.	Cassiterite (631) Naples Yellow (131,335,505) Hematite (1310,223,278) Carbon (1333,1565)	blue yellow, green red,brown black	
<u>OA8435</u>	circa 1700	Lead arsenate (818) Cassiterite (632) Naples Yellow (125,505) Fluorescence (max~600)	blue blue,white,red yellow, green red	Blue: 818 cm ⁻¹ strong Au°?
<u>OA10079</u>	beginning of 18 th c.	Cassiterite (631) Naples Yellow (132,328,450-480-505) Hematite (1315,223,278) Carbon (1333,1565) Lead arsenate (818)	white,blue,green yellow,orange,green orange,red shade (dark yellow) blue	Blue: 818 cm ⁻¹ shoulder
OA6224	2 nd quarter of 18 th c.	Cassiterite (631) Naples Yellow (135,335,450-480-507) Fluorescence (max~600)	white,blue yellow,green red	Au°?
OA8338	2 nd quarter of 18 th c.	Cassiterite (631) Naples Yellow (125,335,504) Lapis Lazuli (542,1086) Carbon (1325,1555) Fluorescence (max~600)	white,blue,purple yellow,green white skin shade purple	Blue: 820 cm ⁻¹ shoulder Au°?
OA8337	Circa 1732-1738	Cassiterite (631) Naples Yellow (125,337,455,508) Carbon (1325,1555) Fluorescence (max~600)	white skin yellow,green shade purple	Au°?

3.1.2 pXRF analysis

Figure 8 shows the characteristic XRF spectra of the metal substrate (OA8435) and the representative enamels (red and green areas) in the full energy window. The intensity depends on the elemental

composition but also the probed volume which is related to the X-ray energy. For instance, the intensity of Cu K_{α} peak is rather similar to that of Au L_{α} and higher than Au L_{β} although the FP semi-quantitative calculated element composition of the metal is $\sim 84\%$ Au, 13% Cu and 1% Ag (wt %). Traces of nickel and iron were also detected. Copper addition is common in order to harden the gold alloy [80]. Silver addition is generally observed in gold applied on ceramics or glass because silver is considered to promote the chemical adhesion with the silicate substrate [81]. Regarding the enamels, measurements are not affected by the contribution of the metal substrate since thickness of the enamel is sufficient to absorb any characteristic X-rays generated by beam interaction of the substrate. Although the silicon content is dominant, corresponding peaks detected at low energy are strongly weakened (measurement in air).

Figures 8 to 10 compare the selected XRF spectra for blue and yellow/green coloured areas in the ~ 5 to 10 (Transition metal energy window), 10 to 13 (detection of As) and 25 to 30 keV (visual comparison of Sn/Sb ratio) range. These limited energy windows allow the comparison of the metal contents associated with the colouring agents such as those of cobalt: Fe, Mn, Ni, Cu, As and Bi; Sb, Sn, Fe, and Zn are indicative of yellow while Co, Cu, Sb, Sn are indicative of green. Table 3 summarizes the major, minor and trace elements detected for different coloured areas of the watches. Sn is observed in almost all the spectra, likely either due to the contribution of the white sub-layer first deposited on gold and/or mixing of cassiterite to adjust the hues. The presence of Sn-rich *Naples yellow* type pigment also contributes to the amount of Sn in the yellow and green areas analysed. Regarding the blue areas analysed, Co is always present in minor amounts, being sufficient to obtain a deep hue. Arsenic always appears to be associated with cobalt, but with different amounts. This outcome seems to be consistent with the As-O signature displaying variable intensities in the Raman spectra recorded: strong intensity observed for OA8435 and OA10079, medium for OA8318, weak for OA10077 and very weak for the others. Significant levels of arsenic were detected by pXRF for the former samples as well as in OA6224 where its Raman spectrum did not show any well-defined As-O peak. This indicates that arsenic could remain dissolved in the glassy silicate network of the enamel, because the saturation limit was not achieved. A TEM study is required to clarify this point. Iron was detected in almost all the blue coloured areas analysed. Levels of impurities such as manganese, nickel, copper and zinc are variable. Small amounts of Bi, also associated with the cobalt ores, was detected as a shoulder on the right side of Pb (L_{α}), As (L_{α}) and Pb (L_{β}) peaks at 10.8 (L_{α}) and 13 (L_{β}) keV for the blue areas of most of the samples analysed (Figure 9).

The first difference observed for yellow and green areas concerns the detection of antimony. It was only well detected in OA8435 which also displays the characteristic Raman signature of Sb-rich

Naples yellow (Figure 4), as mentioned in section 3.1.1. Lower levels of antimony are observed for the yellow of OA10079 (Figure 10) as well as the green and yellow of OA6224 in trace amounts. It was not detected in the other samples. The variable amounts of iron, zinc and copper detected seem to be associated with different compositions of *Naples yellow* type pigment. The spectra exhibiting a rather strong $\sim 335 \text{ cm}^{-1}$ peak together with a significant one at $\sim 480 \text{ cm}^{-1}$ may be correlated to the presence of zinc detected by pXRF (Supplementary Material).

Black areas of OA10077 contain high amounts of manganese and iron which is consistent with the detection of spinel by Raman analysis. In the red areas analysed, gold was well detected for OA8435 and OA6224, due to the colouration by gold nanoparticles. On the contrary, the relatively high amount of iron measured in OA10079 is consistent with the use of hematite, as also detected by Raman scattering (see Supplementary Material).

Light elements such as sodium and boron which are significant components of enamels fired at medium to low temperatures cannot be detected by pXRF in air. Even silicon and aluminium are close to the energy limit of detection, the intensity of their peaks mostly weakened. Potassium was however detected as well as some sulphur.

Table 3: Elements detected in different coloured areas of the enamelled watches; colouring elements in bold.

Inventory number	Date	Colour	XRF major	XRF minor	XRF traces
OA7074	circa 1640	blue yellow green	Pb,Si Pb,Si Pb,Si	Co , <u>Sn</u> , Fe <u>Sn</u> , As, K, Fe K, Cu , <u>Sn</u> , Fe	As, Mn, Ni, Cu, Zn, Zr, Bi Mn, Ni, Cu, Zn, Zr Ti, Mn, Zr
OA10077	mid 17 th c.	blue yellow black	Pb,Si Pb,Si Pb,Si	Co , <u>Sn</u> , Fe Sn , Fe , Zn Mn , Fe , <u>Sn</u>	As, Mn, Ni, Cu, Zn, Bi Mn, Ni, Cu Ni, Cu, Zn, As
OA8435	circa 1700	blue green red metal	Pb,Si Pb,Si Pb,Si Au, Ag, Cu	Co , As, <u>Sn</u> S, Cu , Sb , <u>Sn</u> , Fe, Zn, K Au , <u>Sn</u> , K, Fe	Cu, Zn, Ti, Zr, Bi Mn, Ni, Zr Fe, Ni, Zn, Cu
OA10079	beginning of 18 th c.	blue yellow red	Pb,Si Pb,Si Pb,Si	Co , As, <u>Sn</u> , Fe, Cu Sn , Fe Fe	Mn, Ni Sb, Mn, Ni, Cu, Zn Ni, Cu, Zn
OA6224	2 nd quarter of 18 th c.	Blue green yellow red	Pb,Si Pb,Si Pb,Si Pb,Si	Co , As, <u>Sn</u> , Fe Sn , Zn , Fe , Cu Sn , Zn , Fe <u>Sn</u> , Mn, Zn, Au	Ni, Cu, Zn Ni, Sb Ni, Cu, Sb Fe, Ni

3.2 Glassy matrix

Despite the complex shapes of the background and poor intensity of the Raman spectrum of many types of glassy aluminosilicates, good spectra were recorded in some of the areas analysed, especially on blue (and green) ones due to light absorption which makes the background flatter (Figure 7). The best spectrum was obtained on the green area of OA7074 (Figure 4-bottom) with a broad Si-O bending band peaking at $\sim 500 \text{ cm}^{-1}$ and a broad Si-O stretching band with components between ~ 900 and 1200 cm^{-1} [82-84], as 915 (shoulder), 985 (medium), 1080 (strong) and 1100 (shoulder) cm^{-1} typical of lead-alkali glass [7,21-27,83]. A different signature was observed for OA8435 and OA10079 (more obvious in the blue areas) in which the $\sim 985 \text{ cm}^{-1}$ component becomes stronger (and associated to the strong peak of As-O stretching mode at $\sim 818 \text{ cm}^{-1}$). The higher intensity of the $\sim 985 \text{ cm}^{-1}$ band is consistent with a less polymerized glassy network, indicating a higher lead content required to obtain the precipitation of a lead pyrochlore compound and a lower firing temperature. This finding implies that yellow areas are the last to be painted and fired. It can be concluded that the compositions of the enamel matrix are almost similar for all studied artefacts, except for blue areas and yellow areas for which significant characteristics can be identified. At least, three cycles of firing are thus required.

4. Discussion

Both Raman microspectroscopy and pXRF showed that a mixture of different pigments had been used for all hues of the enamelled decor, painted after the deposit of a white layer opacified primarily with cassiterite, according to the ancient receipts [28-30]. This outcome sheds light on the technique of watch enamellers which is in a way similar to that of oil and tempera painters, contrarily to the common procedure used by glass and metal enamellers. The latter craftsmen had preferred to make a superimposition of coloured layers to adjust the hues of the decor [8,85]. Figure 11 shows the comparison of the decors of OA7074 (circa 1640) and OA6224 (2nd quarter of the 18th century) at high optical magnification (x5 times) where differences in the painting technique are obvious. The 17th century decor shows the application of nearly horizontal brush strokes and colour fillets while the 18th century one shows a superposition of small dots of colour on the plates, similar to what is observed in the miniature drawings and 'gouache' painting. Raman analysis was performed at very local scale, much smaller than the coloured dots. Thus, the laser spot could analyse a homogeneous region in both types of the decor within visual perception. Nevertheless, a combination of pigments was detected, for instance in OA6224 where the intensity of the cassiterite doublet increases when the focus is displaced from the enamel surface to the substrate (Figure 4-top, yellow 1 to yellow 2). This finding is related to the very first painting of a white layer on which the decor would be painted. Similar observation was made for the yellow of OA7074 (Figure 4-bottom, yellow 3 to yellow 1),

green of OA8337 (Figure 4-bottom, bottom to top spectrum), dark blue of OA8435 (Figure 4-top, top to bottom spectrum), green of OA8338 (Figure 6, top to bottom spectrum) and yellow of OA8318 (Figure 6, bottom to top spectrum) as well as many other colours (Supplementary Material). Mixing pigments was also used to adjust the shade, for instance the strongest peak of *Naples Yellow* type pigment was detected in the blue areas of OA10079 and OA10077 (Figure 7). Furthermore, addition of hematite is common, as in the green of OA7074 (Figure 4-bottom) (note the strongest band of hematite at $\sim 1310 \text{ cm}^{-1}$). Hematite was obviously added to obtain the green hue due to the lack of thermostable green pigments before the mastering of chromium derivatives at the end of the 18th century in Europe [60]. The complex colour of the skin/white of the figures was also obtained by small additions of *Naples Yellow* type pigment in OA6224 (Figure 4-top) and OA8338 (Figure 6) as well as lapis lazuli in OA8338 (Figure 6, if not a restoration?).

The presence of some types of pigments seems to be correlated to the date of production. The significant amount of arsenic in blue areas is consistent with the use of As-rich cobalt ores (Table 2), as typically observed for 17th century European artefacts, namely Limoges enamels [7], blue-and-white soft-paste porcelains [33] as well as blue trade beads [86-88]. Arsenic-rich cobalt ores, mainly from the Erzgebirge mountains of Saxony [70,89-91], namely (Schneeberg, Johann-Georgenstadt, Annaberg)[90,91] but also from Sainte-Marie-aux-Mines (Vosges, France), Gifthain (Pyrénées, France)[90] and Sweden [91] were mined during the 17th and 18th centuries. Ores coming from these mining activities are secondary deposits issued from hydrothermal veins characterised by a high level of arsenic ($\text{As/Co} \gg 1$) in association with nickel, silver and bismuth [91]. On the contrary, Asian ores are primary deposits rich in iron and manganese [70]. Up to the middle of the 16th century, cobalt was a by-product of silver mining and the preparation route almost eliminated all the arsenic content, but also partly bismuth [90]. The higher demand of cobalt used as a common colourant for glass, ceramics as well as oil paintings then led to the mining of specifically cobalt ores after the middle of the 16th century. Regarding white, grey, blue, red or black cobalt ores; pieces are visually selected, ground, sifted and grinded. The firing process results in the elimination of a large part of arsenic which is a volatile element. Usually, the cobalt-rich matter is mixed with variable quantities of quartz, sand or flint and potash and then melted to obtain different grades of smalt, a potash glass coloured in blue. The resulting smalt undergoes the processes of powdering, sifting, washing and is then classified [90]. It is worth mentioning that for enamelling, due to the thinness of the layer, "cobalt-richer" grades are required, much richer than those used for the colouration of glass. Typically, 0.3 % to 1 % wt cobalt is required for enamel, a much lower amount being sufficient for a glass object. The final composition thus depends not only on the mineral(s) and the mining location but also on the preparation procedure.

The analytical studies of Limoges enamels identified the use of As-rich ores for high quality productions (Limosin and Laudin workshops) and As-free ores (more precisely not Raman detected) for common ones (Nouailher workshop) [7]. This indicates that craftsmen had recognized the advantage of As-containing cobalt ores to prepare high quality enamels and too purified ingredients are not the most efficient but perhaps less expensive (and less concentrated in cobalt). In fact, the addition of arsenic was made voluntarily in 18th century productions [74]. However, traces of arsenic were detected in the watch enamels in which the Raman technique did not detect the As-O bond (e.g. OA7074) or detection is difficult (OA10077). Quantitative measurements and mapping are required in order to confirm whether arsenic remains dissolved in the glassy matrix because the saturation limit was not obtained due to the relatively low content or modification of the composition of the glassy matrix. Another possibility could be that heterogeneity was not detected with our measurement procedures based on three spots.

The specific Raman spectral background signature with a maximum at ~550 nm indirectly indicating the presence of colloidal gold, also confirmed by pXRF for the samples analysed, was particularly observed for the artefacts produced after 1640, the time corresponding to the period of ruby glass production by Bernard Perrot [15,16,78]. Two different techniques of colloidal gold preparation are known; firstly, the Perrot's technique using arsenic for the precipitation of Au⁰ nanoparticles from mother acid solution [15,78] and later the Kunckel's technique by the addition of tin [15,78,79]. The mixing with cassiterite and poor intensity of Raman components prevent the precise identification of the procedure used, except for the spectra collected on the purple areas of OA8338 where a shoulder at ~810 cm⁻¹ characteristic of the As-O mode suggests the utilization of Perrot's technique (Figure 6). Obviously, a larger corpus of watches is needed to unambiguously establish the time for the first use of colloidal gold as red chromophore in the enamelled watches. Yet, it seems that watch enamellers had used the technique very early as glassmakers, earlier than potters.

It seems difficult to associate the composition of *Naples Yellow* type pigment with the date of the artefacts due to the small corpus studied and the fact that complex lead pyrochlore solid solutions had been extensively used in the Western/Mediterranean countries since the Roman period [69]. The variation of a pigment's composition can be a criterion for workshop identification [43-45,62,63,66-68,92-94]. However, Sb-rich *Naples yellow* compositions were not observed for the 17th century watches in general. The variable contents of iron and zinc detected by pXRF seem to be characteristic of the 18th century enamels and clearly demonstrate that different compositions of the pigment had been used. Thus, combination of quantitative XRF and Raman analyses may offer a more useful and precise method to trace productions from the same workshop.

4. Conclusions

This preliminary work about the 17th-18th century enamelled watches, mostly produced in France, confirms the efficiency of the combination of Raman and XRF mobile set-ups to obtain technical information on enamelled objects. Thickness of the enamel appears to be sufficient to avoid (most of) the contamination of pXRF data by the contribution of the metal substrate. The results suggest that technological changes both for the enamel painting technique and the pigment preparation began at the turn of the 17th – 18th century. The abandonment of the use of As-rich cobalt ores for blue enamels is significant for the 18th century, arsenic being at level below its precipitation limit. The invention of red/purple/violet colour preparation with Au⁰ nanoparticles also emerged after the middle of the 17th century, at the same period when Bernard Perrot started to produce ruby glass, but before the use of 'Cassius' purple for glazed pottery; in one of the samples, detection of the As-O bond indicates that Perrot's procedure had been used. Rather similar glassy matrices were observed for all the enamels, except for blue and yellow/green areas where the use of cobalt chromophore and *Naples yellow* type pigment modifies the enamel matrix. Raman analysis from the surface to the inner layer gives information about the superimposition of colour touches. Contrarily to Limoges enamels, the hue palette deposited by the pencil consists of intimate mixture of pigments, as in the case of easel oil paintings. Examination of a higher number of objects and more sophisticated data treatment will contribute to a more detailed view of the evolution of enamelling technology during the 17th-18th centuries.

Acknowledgments

Mrs. Véronique Schloupt from France Scientifique is kindly acknowledged for providing the mobile XRF instrument. Dr. Céline Paris is kindly acknowledged for her help in recording some data.

Figure Captions

Fig. 1: Enamelled watches from Musée du Louvre, Paris collection: a) OA8428, circa 1640 (Robert Chevallier?); b) OA8429, circa 1630-1640 (Robert Chevallier); c) OA7074, circa 1640; d) OA8318, mid-17th century; e) OA8338, 2nd quarter of the 18th century (Decombaz).

Fig. 2: Enamelled watches from Musée du Louvre, Paris collection: a) OA7075, mid-17th century (Jean II Toutin); b) OA10077, mid-17th century (attributed to Robert Vauquer); c) OA10079, beginning of the 18th century (F. Braun); d) OA8435, circa 1700.

Fig. 3: Enamelled watches from Musée du Louvre, Paris collection: a) OA8432, last quarter of 17th century; b) OA8337, circa 1732-1738; c) OA6224, 2nd quarter of the 18th century.

Fig. 4: Representative Raman spectra recorded on OA8435, OA8337, OA6224 and OA7074 enamelled watches (see Supplementary Material for details).

Fig. 5: Comparison of Raman spectra recorded on yellow (and green) areas.

Fig. 6: Representative Raman spectra recorded on OA8338 (2nd quarter of the 18th c.) and OA8318 (mid 17th c.) enamelled watches (see Supplementary Material for details).

Fig. 7: Comparison of Raman spectra recorded on blue (left) and red-to-purple (right) areas.

Fig. 8. Representative pXRF spectra recorded on (top) the metal substrate (OA8435), green and red enamels. Details of selected energy windows are shown in Figs 9 and 10.

Fig. 9. Representative pXRF spectra recorded in blue areas for energy windows characteristic of the companion elements of cobalt ores.

Fig. 10. Representative pXRF spectra recorded in yellow and green areas for energy windows characteristic of elements that could incorporate into the lead pyrochlore solid solution.

Fig. 11. Comparison of the painting technique of the 17th (top) and 18th century (bottom) enamels.

References

- [1] A. Pierides, *Jewellery in the Cyprus Museum*, Republic of Cyprus the Department of Antiquities, Cyprus, 1971.
- [2] M.-M. Gauthier, Émaux, in *Encyclopedia Universalis*, vol. 6, Paris, 1985, pp. 939-960.
- [3] E. Cooper, *Ten Thousand Years of Pottery* (4th edition), University of Pennsylvania Press, Philadelphia, 2000.
- [4] V. Kruta, The first Celtic expansion: prehistory to history, in S. Moscati, P. Grassi, V. Mario Andreose, C. Tanzi (Eds.), *The Celts*, Bompiani, Milano, 1991, pp. 195-210.
- [5] M.-J. Roulière-Lambert (Ed.), *Les émaux celtiques*, Centre Jurassien du Patrimoine, Lons-le-Saunier, 2008.
- [6] O.M. Dalton, *Byzantine Art and Archaeology*, Dover Publications, NY, 1961.
- [7] Ph. Colomban, L. Arberet, B. Kirmizi, On-site Raman analysis of 17th and 18th century Limoges enamels: Implications on the European cobalt sources and the technological relationship between Limoges and Chinese enamels, *Ceram. Int.* 43 (13) (2017) 10158-10165.
- [8] B. Kirmizi, Ph. Colomban, B. Quette, On-site analysis of Chinese Cloisonné enamels from fifteenth to nineteenth centuries, *J. Raman Spectrosc.* 41 (7) (2010) 780–790.
- [9] Ph. Colomban, A. Tournié, M.C. Caggiani, C. Paris, Pigments and enamelling/gilding technology of Mamluk mosque lamps and bottle, *J. Raman Spectrosc.* 43 (12) (2012) 1975-1984.
- [10] M.C. Caggiani, Ph. Colomban, C. Valotteau, A. Mangone, P. Cambon, Mobile Raman spectroscopy analysis of ancient enamelled glass masterpieces, *Anal. Methods* 5 (2013) 4345-4354.
- [11] R. Ward, *Gilded and Enamelled Glass from the Middle East*, British Museum Press, London, 1998.
- [12] S. Carboni, *Glass from Islamic Lands: The Al-Sabah Collection at the Kuwait National Museum*, Thames & Hudson, London, 2001.
- [13] P. McCray (Ed.), *Prehistory and History of Glassmaking Technology*, Ceramics and Civilization Series Volume VIII, The American Ceramic Society, Westerville, 1998.
- [14] I. C. Freestone, The relationship between enamelling on ceramics and on glass in the Islamic world, *Archaeometry* 44 (2) (2002) 251-255.
- [15] J. Bénard, B. Dragesco (Eds), *Bernard Perrot et les verreries royales du Duché d’Orléans, 1662-1754*, Editions des Amis du musée d’Orléans, Orléans, 1989.
- [16] Ph. Colomban, B. Kirmizi, Non-invasive on-site Raman study of polychrome and white enamelled glass artefacts in imitation of porcelain assigned to Bernard Perrot and his followers, *J. Raman Spectrosc.* 51 (1) (2020) 133-146.
- [17] K. H.A. Janssens (Ed.), *Modern Methods for Analysing Archaeological and Historical Glass*, John Wiley & Sons, First Edition, 2 Vol., Chichester, 2013.
- [18] W. D. Kingery, Painterly maiolica of the Italian Renaissance, *Techn. & Cult.* 34 (1) (1993) 28-48.
- [19] P. Verdier, *Catalogue of the Painted Enamels of the Renaissance*, Baltimore, 1967.
- [20] M. Blanc, I. Biron, Ph. Colomban, V. Notin, *Emaux peints de Limoges, XVe-XVIIIe siècles – La collection du Musée des arts décoratifs*, Les Arts Décoratifs, Paris, 2011.
- [21] B. Kirmizi, Ph. Colomban, M. Blanc, On-site analysis of Limoges enamels from sixteenth to nineteenth centuries: an attempt to differentiate between genuine artefacts and copies, *J. Raman Spectrosc.* 41 (10) (2010) 1240–1247.

- [22] M. Perez y Jorba, M. Rommeluere, C. Bahezre, Microstructure d'une plaque d'émail peint de Limoges du XVI^e siècle, *Stud. Conserv.* 36 (2) (1991) 76–84.
- [23] M.T. Wypyski, R.W. Richter, Preliminary compositional study of 14th and 15th century European enamels, *Techné* 6 (1997) 48–57.
- [24] S. Röhrs, H. Stege, Analysis of Limoges painted enamels from the 16th to 19th centuries by using a portable micro X-ray fluorescence spectrometer, *X-Ray Spectrom.* 33 (6) (2004) 396–401.
- [25] C. Cardinal, *La montre des origines au XIX^e siècle*, Office du Livre, Fribourg, 1985.
- [26] C. Cardinal, *La collection des montres et horloges de table du musée du Louvre*, Tome 1 (1984); tome 2 (2000), RMN, Paris.
- [27] C. Cardinal, L'horloge, un objet emblématique de la Renaissance, in *Trésors d'horlogerie. Le temps et sa mesure du Moyen-Age à la Renaissance*, Editions RMG/Palais des Papes, Avignon, 1998.
- [28] A. Félibien, De la peinture en émail, in *Des principes de l'architecture, de la sculpture, de la peinture et des autres arts qui en dépendent, avec un dictionnaire des termes propres à chacun de ces arts*, 2nd Edition, Jean-Baptiste Coignard, Paris, 1690, pp. 426-437.
- [29] D. d'Arclais de Montamy, *Traité des couleurs pour la peinture en émail et sur la porcelaine, précédé de l'art de peindre sur l'émail*, P.G. Le Mercier, Paris, 1765.
(https://data.bnf.fr/fr/12375580/didier_d_arclais_de_montamy/ accessed 15th December 2019)
- [30] H. Bertran, Reboulleau, Magnier, A. Romain, *Nouveau Manuel Complet de la peinture sur verre, sur porcelaine et sur émail*, Encyclopédie-Roret, L. Mulo, Paris, 1913.
- [31] F. Lili, *La céramique chinoise*, China Intercontinental Press, Beijing, 2011.
- [32] B. Zhao, G. Wang, I. Biron, Ph. Colomban, L. Hilaire-Pérez, La circulation des techniques de l'émail entre la France et la Chine du XVII^e au XIX^e siècle, *Le CNRS en Chine Bulletin* 21 (2016) 20–25.
(http://www.cnrs.fr/derci/IMG/pdf/cnrsenchine_21_fr_final_pour_le_site_cnrs.pdf, accessed 15th December 2019).
- [33] Ph. Colomban, T.-A. Lu, V. Milande, Non-invasive on-site Raman study of blue-decorated early soft-paste porcelain: the use of arsenic-rich (European) cobalt ores – Comparison with *huafalang* Chinese porcelains, *Ceram. Int.* 44 (8) (2018) 9018-9026.
- [34] Ph. Colomban, F. Ambrosi, A.-T. Ngo, T.-A. Lu, X.-L. Feng, S. Chen, C.-L. Choi, Comparative analysis of *wucai* Chinese porcelains using mobile and fixed Raman microspectrometers, *Ceram. Int.* 43 (16) (2017) 14244-14256.
- [35] R. Giannini, I.C. Freestone, A.J. Shortland, European cobalt sources identified in the production of Chinese *famille rose* porcelain, *J. Archaeol. Sci.* 80 (2017) 27–36.
- [36] Ph. Colomban, B. Zhao, J.-B. Clais, B. Kirmızı, V. Droguet, Non-invasive on-site Raman study of pigments and glassy matrix of the 17th-18th century painted enamelled Chinese metal wares: Comparison with French enamelling technology, *Coatings*, submitted.
- [37] Ph. Colomban, The on-site/remote Raman analysis with mobile instruments: a review of drawbacks and success in cultural heritage studies and other associated fields, *J. Raman Spectrosc.* 43 (11) (2012) 1529-1535.
- [38] Ph. Colomban, On-site Raman study of artwork: Procedure and illustrative examples, *J. Raman Spectrosc.* 49 (6) (2018) 921-934.

- [39] J.M. Madariaga, Analytical chemistry in the field of cultural heritage, *Anal. Methods* 7 (12) (2015) 4848-4876.
- [40] P. Vandenabeele, H.G.M. Edwards, J. Jehlička, The role of mobile instrumentation in novel applications of Raman spectroscopy: archaeometry, geosciences, and forensics, *Chem. Soc. Rev.* 43 (8) (2014) 2628-2649.
- [41] Y. Su, L. Qu, H. Duan, N. Tarcea, A. Shen, J. Popp, J. Hu, Elemental analysis-aided Raman spectroscopic studies on Chinese cloisonné wares and painted enamels from the Imperial palace, *Spectrochim. Acta A-Mol. Biomol. Spectrosc.* 153 (2016) 165–170.
- [42] J. Henderson, M. Tregear, N. Wood, The technology of sixteenth- and seventeenth century Chinese Cloisonné enamels, *Archaeometry* 31 (2) (1989) 133–146.
- [43] R. Montanari, M.F. Alberghina, A. Casanova Municchia, E. Massa, A. Pelagotti, C. Pelosi, S. Schiavone, A. Sodo, A polychrome Mukozuke (1624–1644) porcelain offers a new hypothesis on the introduction of European enameling technology in Japan, *J. Cult. Herit.* 32 (2018) 232-237.
- [44] R. Montanari, N. Murakami, M.F. Alberghina, C. Pelosi, S. Schiavone, The Origin of overglaze-blue enameling in Japan: New discoveries and a reassessment, *J. Cult. Herit.* 37 (2019) 94–102.
- [45] R. Montanari, N. Murakami, Ph. Colomban, M. F. Alberghina, C. Pelosi, S. Schiavone, European Ceramic technology in the Far East: Enamels and pigments in Japanese art from the 16th to the 20th century and their reverse influence on China, submitted.
- [46] M. Giarola, G. Mariotto, M. Barberio, D. Ajo, Raman spectroscopy in gemmology as seen from a 'jeweller's' point of view, *J. Raman Spectrosc.* 43 (11) (2012) 1828-1832.
- [47] Z. Petrova, J. Jehlička, T. Capoun, R. Hanus, T. Trojek, V. Golias, Gemstones and noble metals adorning the sceptre of the Faculty of Science of Charles University in Prague: integrated analysis by Raman and XRF handheld instruments, *J. Raman Spectrosc.* 43 (9) (2012) 1275-1280.
- [48] E.M.A. Ali, H.G.M. Edwards, Analytical Raman spectroscopy in a forensic art context: The non-destructive discrimination of genuine and fake lapis lazuli, *Spectrochim. Acta A-Mol. Biomol. Spectrosc.* 121 (2014) 415-419.
- [49] G. Barone, D. Bersani, P.P. Lottici, P. Mazzoleni, S. Raneri, U. Longobardo, Red gemstone characterization by micro-Raman spectroscopy: the case of rubies and their imitations, *J. Raman Spectrosc.* 47 (12) (2016) 1534-1539.
- [50] G. Barone, P. Mazzoleni, S. Raneri, J. Jehlička, P. Vandenabeele, P.P. Lottici, G. Lamagna, A.M. Manenti, D. Bersani, Raman Investigation of Precious Jewelry Collections Preserved in Paolo Orsi Regional Museum (Siracusa, Sicily) Using Portable Equipment, *Appl. Spectrosc.* 70 (9) (2016) 1420-1431.
- [51] M. Aceto, E. Agosta, A. Arrais, E. Cala, E. Mazzucco, S. Lomartire, A. Agostino, G. Fenoglio, Multi-technique characterization of adhesives used in medieval jewellery, *Archaeometry* 59 (6) (2017) 1105-1118.
- [52] J. Jehlička, A. Culka, M. Bastova, P. Basta, J. Kuntos, The Ring Monstrance from the Loreto treasury in Prague: handheld Raman spectrometer for identification of gemstones, *Phil. Trans. A Math. Phys. Eng. Sci.* 374 (2082) (2016) 1-19.
- [53] A. Culka, J. Jehlička, Identification of gemstones using portable sequentially shifted excitation Raman spectrometer and RRUFF online database: A proof of concept study, *Eur. Phys. J. Plus* 134 (4) (2019) 130.
- [54] A. Culka, J. Jehlička, A database of Raman spectra of precious gemstones and minerals used as cut gems obtained using portable sequentially shifted excitation Raman spectrometer, *J. Raman Spectrosc.* 50 (2) (2019) 262-280.

- [55] I. Tisso, M. Manso, M. F. Guerra, Unveiling the art of René Lalique with XRF and Raman spectroscopy - Technological innovation in jewellery production, *J. Cult. Herit.* 33 (2018) 83-89.
- [56] C. Cardinal, Les peintres sur émail au temps de l'atticisme. Des tondi servant de modèles à la décoration des montres, in: L. Riviale & J.F. Luneau (Eds.), *L'Invention partagée*, Presse Universitaires Blaise Pascal, Clermont-Ferrand, 2019, pp. 303-320.
- [57] C. Zum Kolk, La sédentarisation de la cour à Paris d'après les itinéraires des derniers Valois (1515-1589), in: B. Bove, M. Gaude-Ferragu, C. Michon (Eds.), *Paris, ville de cour (XIIIe-XVIIIe siècle)*, PUR, Rennes, 2017. (<https://hal.archives-ouvertes.fr/hal-01829675/> accessed 15th December 2019)
- [58] P. Joutard, Réseaux huguenots et espace Européen (XVI^e–XXI^e siècle), *Rev. synth.* 123 (1) (2002) 111-129. (<https://doi.org/10.1007/BF02963323> /accessed 15th December 2019)
- [59] Ph. Colomban, V. Milande, L. Le Bihan, On-site Raman analysis of Iznik pottery glazes and pigments, *J. Raman Spectrosc.* 35 (7) (2004) 527-535.
- [60] Ph. Colomban, G. Sagon, X. Faurel, Differentiation of Antique Ceramics from the Raman Spectra of their Colored Glazes and Paintings, *J. Raman Spectrosc.* 32 (5) (2001) 351-60.
- [61] Ph. Colomban, Lapis lazuli as unexpected blue pigment in Iranian Lâjvardina ceramics, *J. Raman Spectrosc.* 34 (6) (2003) 420-423.
- [62] C. Sandalinas, S. Ruiz-Moreno, Lead-tin-antimony yellow-Historical manufacture, molecular characterization and identification in seventeenth-century Italian paintings, *Stud. Conserv.* 49 (1) (2004) 41–52.
- [63] C. Sandalinas, S. Ruiz-Moreno, A. Lopez-Gil, J. Miralles, Experimental confirmation by Raman spectroscopy of a Pb-Sn-Sb triple oxide yellow pigment in sixteenth-century Italian pottery, *J. Raman Spectrosc.* 37 (10) (2006) 1146–1153.
- [64] P. Ricciardi, Ph. Colomban, A. Tournié, V. Milande, Non-destructive on-site identification of ancient glasses: genuine artefacts, embellished pieces or forgeries?, *J. Raman Spectrosc.* 40 (6) (2009) 604–617.
- [65] M. Pereira, T. de Lacerda-Aroso, M.J.M. Gomes, A. Mata, L.C. Alves, Ph. Colomban, Ancient Portuguese ceramic wall tiles («Azulejos»): characterization of the glaze and ceramic pigments, *J. Nano Res.* 8 (2009) 79–88.
- [66] F. Rosi, V. Manuali, C. Miliani, B.G. Brunetti, A. Sgamellotti, T. Grygar, D. Hradil, Raman scattering features of lead pyroantimonate compounds. Part I: XRD and Raman characterization of Pb₂Sb₂O₇ doped with tin and zinc, *J. Raman Spectrosc.* 40 (1) (2009) 107–111.
- [67] C. Pelosi, G. Agresti, U. Santamaria, E. Mattei, Artificial yellow pigments: production and characterization through spectroscopic methods of analysis, *e-Preservation Science* 7 (2010) 108–115.
- [68] B. Kırmızı, H. Göktürk, Ph. Colomban, Colouring agents in the pottery glazes of western Anatolia: a new evidence for the use of Naples yellow pigment variations during the late Byzantine period, *Archaeometry* 57 (3) (2015) 476–496.
- [69] E. Neri, C. Morvan, Ph. Colomban, M.F. Guerra, V. Prigent, Late Roman and Byzantine mosaic opaque “glass-ceramics” tesserae (5th–9th century), *Ceram. Int.* 42 (16) (2016) 18859–18869.
- [70] Ph. Colomban, Rocks as blue, green and black pigments/dyes of glazed pottery and enamelled glass artefacts –A review, *Eur. J. Mineral.* 25 (5) (2014) 863–879.
- [71] M.T. Vandenborre, E. Husson, Comparison of the force field in various pyrochlore families. I. The A₂B₂O₇ oxides, *J. Solid State Chem.* 50 (3) (1983) 362–371.

- [72] M.T. Vandenborre, E. Husson, Comparison of the force field in various pyrochlore families. II. Phases presenting structural defects, *J. Solid State Chem.* 53 (2) (1984) 253–259.
- [73] K. Sakellariou, C. Miliani, A. Morresi, M. Ombelli, Spectroscopic investigation of yellow majolica glazes, *J. Raman Spectrosc.* 35 (1) (2004) 61–67.
- [74] M. Maggetti, A. d’Albis, Phase and compositional analysis of a Sèvres soft paste porcelain plate from 1781, with a review of early porcelain techniques, *Eur. J. Mineral.* 29 (3) (2017) 347–367.
- [75] B. Manoun, M. Azdouz, M. Azrour, R. Essehli, S. Benmokhtar, L. El Ammari, A. Ezzahi, A. Ider, P. Lazor, Synthesis, Rietveld refinements and Raman spectroscopic studies of tricationic lacunar apatites $\text{Na}_{1-x}\text{K}_x\text{Pb}_4(\text{AsO}_4)_3$ ($0 < x < 1$), *J. Mol. Struct.* 986 (1-3) (2011) 1–9.
- [76] J. Van Pevenage, D. Lauwers, D. Herremans, E. Verhaeven, B. Vekemans, W. De Clercq, L. Vincze, L. Moens, P. Vandenabeele, A combined spectroscopic study on Chinese porcelain containing *ruan-cai* colours, *Anal. Methods* 6 (2) (2014) 387–394.
- [77] F. Froment, A. Tournié, Ph. Colomban, Raman identification of natural red to yellow pigments: ochre and iron-containing ores, *J. Raman Spectrosc.* 39 (5) (2008) 560–568.
- [78] J. Geysant, Secret du verre rouge transparent de Bernard Perrot et comparaison avec celui de Johann Kunckel, in: Bernard Perrot (1640-1709): Secrets et chefs-d’œuvre des verreries royales d’Orléans, Catalogue, Musée des Beaux-Arts d’Orléans, SOMOGY Editions d’Arts, Paris, 2010, pp. 51-54.
- [79] C. Louis, Gold nanoparticles in the past: Before the Nanotechnology Era, in: C. Louis, O. Pluchery (Eds.), *Gold Nanoparticles for Physics, Chemistry and Biology*, Imperial College Press, London, 2012, pp. 1-27.
- [80] N. Sougy, Liberté, légalité, qualité : le luxe des produits d’or et d’argent à Genève au XIXe siècle, *Entreprises et Histoire* 46 (1) (2007) 71-84.
- [81] Ph. Colomban, T. Calligaro, C. Vibert-Guigue, Q. L. Nguyen, H.G.M. Edwards, Dorures des céramiques et tesselles anciennes : technologies et accrochage, *ArcheoSciences – Rev. Archeom.* 29 (2005) 7-20.
- [82] Ph. Colomban, Polymerization degree and Raman identification of ancient glasses used for jewellery, ceramic enamels and mosaics, *J. Non-Cryst. Solids* 323 (1-3) (2003) 180–187.
- [83] Ph. Colomban, A. Tournié, L. Bellot-Gurlet, Raman identification of glassy silicates used in ceramic, glass and jewellery: a tentative differentiation guide, *J. Raman Spectrosc.* 37 (8) (2006) 841–852.
- [84] Ph. Colomban, Non-destructive Raman analysis of ancient glasses and glazes, in: K. Janssens (Ed.), *Modern Methods for Analysing Archaeological and Historical Glass 2*, First Edition, John Wiley & Sons Ltd, Hoboken, 2012, pp. 275–300 (ch. 4.2).
- [85] Ph. Colomban, M. Maggetti, A. d’Albis, Non-invasive Raman identification of crystalline and glassy phases in a 1781 Sèvres Royal Factory soft paste porcelain plate, *J. Eur. Ceram. Soc.* 38 (15) (2018) 5228–5233.
- [86] R.G.V. Hancock, J. McKechnie, S. Aufreiter, K. Karklins, M. Kapches, M. Sempowski, J.-F. Moreau, I. Kenyon, Non-destructive analysis of European cobalt blue glass trade beads, *J. Radioanal. Nucl. Chem.* 244 (3) (2000) 567–573.
- [87] A. Bonneau, J.-F. Moreau, R. Auger, R.G.V. Hancock, B. Émard, Analyses physico-chimiques des perles de traite en verre de facture européenne: quelles instrumentations pour quels résultats?, *Archéologiques* 26 (2014) 109–132.

- [88] F. Koleini, Ph. Colomban, I. Pikirayi, L.C. Prinsloo, Glass beads, markers of ancient trade in sub-Saharan Africa: Methodology, state of the art and perspectives, *Heritage* 2 (3) (2019) 2343–2369; doi:10.3390/heritage2030144.
- [89] B. Gratuze, I. Soulier, M. Blet, L. Vallauri, De l'origine du cobalt: du verre à la céramique, *ArcheoSciences- Rev. Archeom.* 20 (1996) 77-94.
- [90] M. Valmont de Bomare, *Minéralogie, ou nouvelle exposition du règne minéral*, 2^{nde} Edition, Vol. 2, Vincent Imprimeur-Libraire, Paris, 1774, pp. 76-96.
- [91] S.A. Kissin, Five element (Ni-Co-As-Ag-Bi) veins, *Geosci. Can.* 19 (3) (1992) 113-124. (<https://journals.lib.unb.ca/index.php/gc/article/view/3768/4282> /accessed 15th December 2019).
- [92] J. Dik, E. Hermens, R. Peschar, H. Schenk, Early production recipes for lead antimonate yellow in Italian art, *Archaeometry* 47(3) (2005) 593–607.
- [93] G. Agresti, P. Baraldi, C. Pelosi, U. Santamaria, Yellow pigments based on lead, tin and antimony: ancient recipes, synthesis, characterization and hue choice in artworks, *Colour Res. Appl.* 41 (3) (2016) 226-231.
- [94] L. Cartechini, F. Rosi, C. Miliani, F. D'Acapito, B.G. Brunetti, A. Sgamellotti, Modified Naples yellow in Renaissance majolica: study of Pb-Sb-Zn and Pb-Sb-Fe ternary pyroantimonates by X-ray absorption spectroscopy, *J. Anal. At. Spectrom.* 26 (12) (2011) 2500-2507.



Fig. 1: Enamelled watches from Musée du Louvre, Paris collection: a) OA8428, circa 1640 (Robert Chevallier?); b) OA8429, circa 1630-1640 (Robert Chevallier); c) OA7074, circa 1640; d) OA8318, mid-17th century; e) OA8338, 2nd quarter of the 18th century (Decombaz).



Fig. 2: Enamelled watches from Musée du Louvre, Paris collection: a) OA7075, mid-17th century (Jean II Toutin); b) OA10077, mid-17th century (attributed to Robert Vauquer); c) OA10079, beginning of the 18th century (F. Braun); d) OA8435, circa 1700.

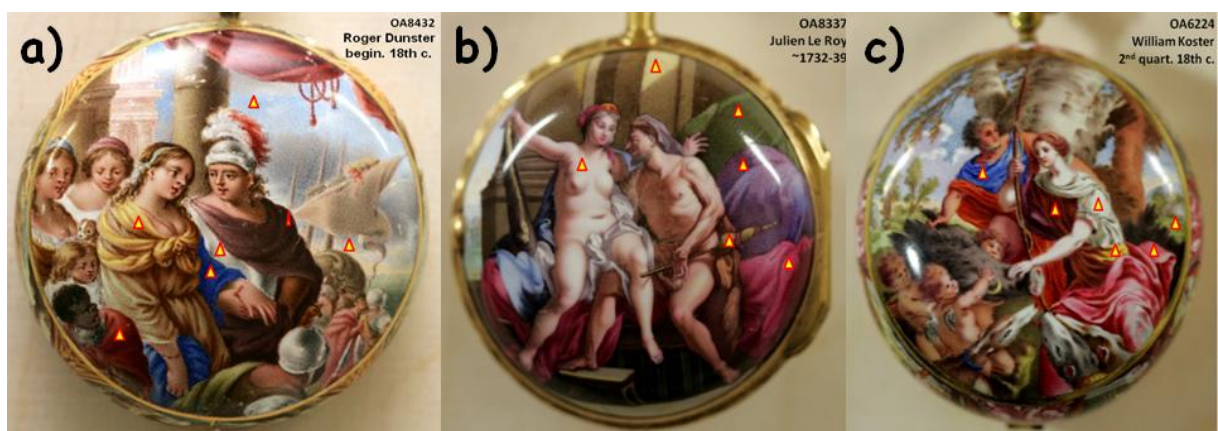


Fig. 3: Enamelled watches from Musée du Louvre, Paris collection: a) OA8432, last quarter of 17th century; b) OA8337, circa 1732-1738; c) OA6224, 2nd quart. of the 18th century.

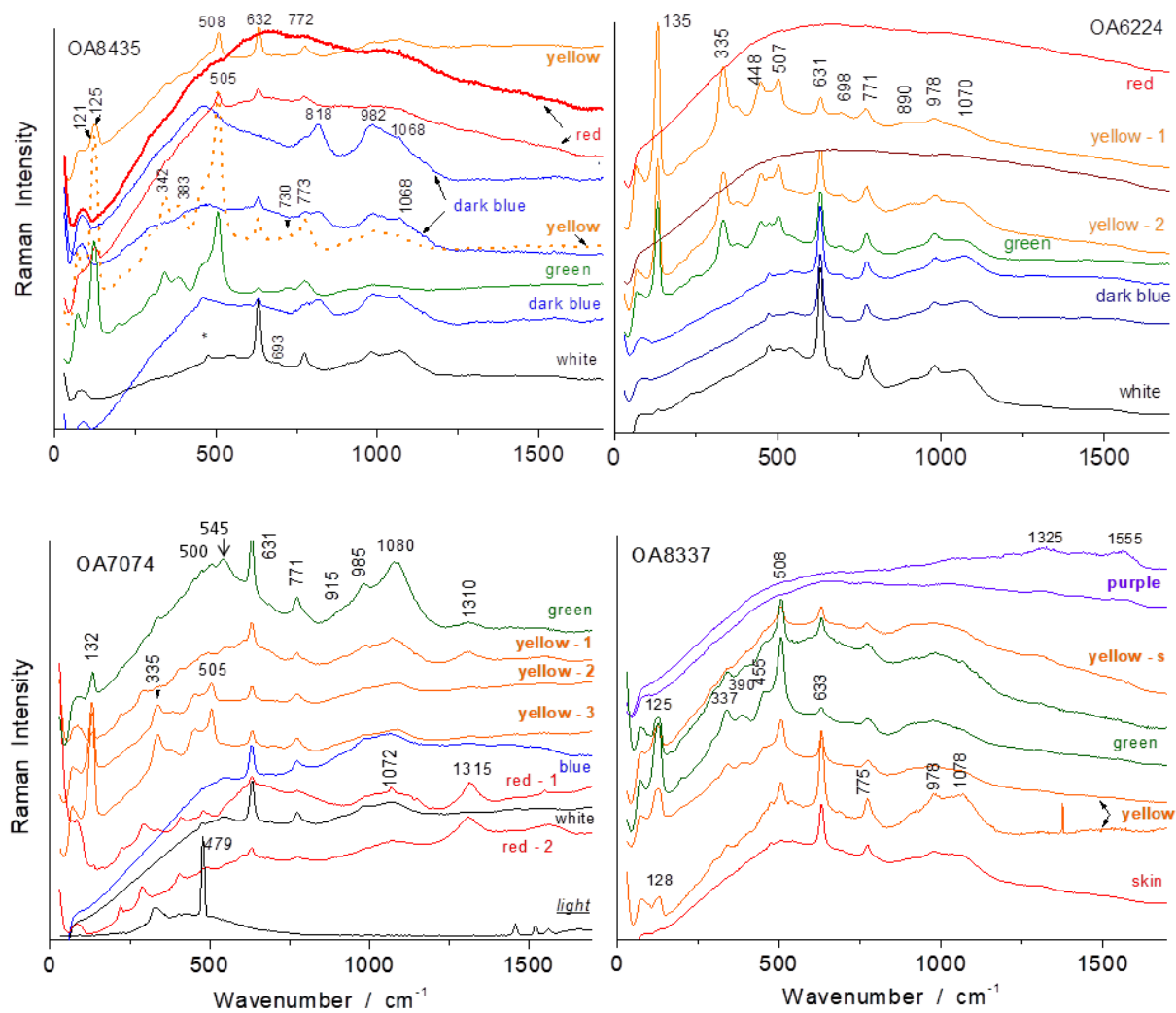


Fig. 4: Representative Raman spectra recorded on OA8435, OA8337, OA6224 and OA7074 enamelled watches (see Supplementary Material for details).

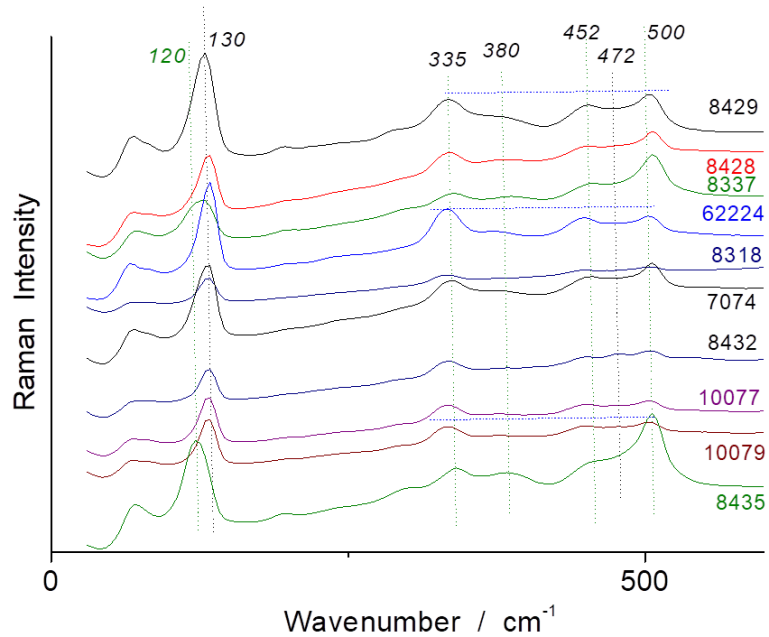


Fig. 5: Comparison of Raman spectra recorded on yellow (and green) areas.

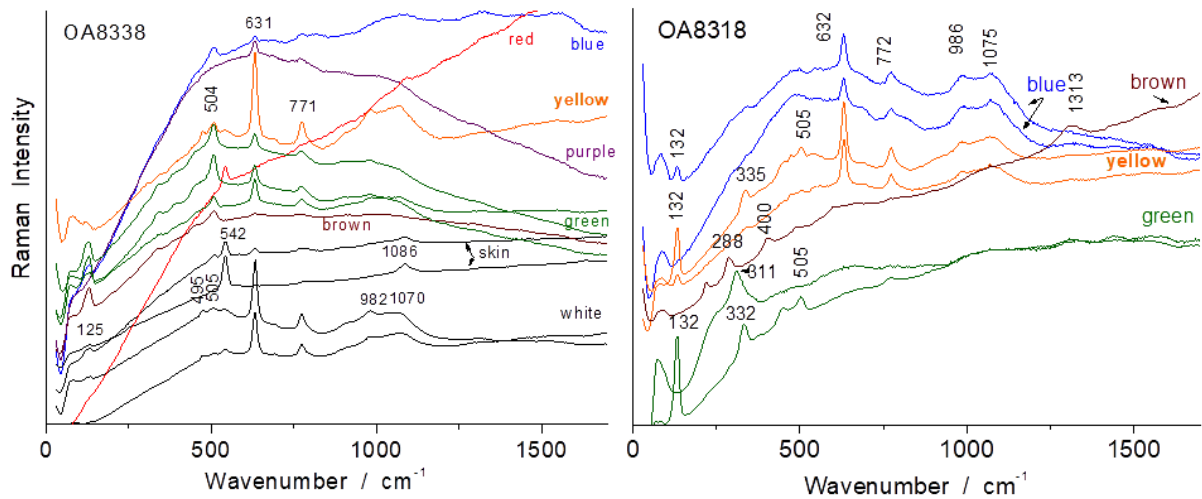


Fig. 6: Representative Raman spectra recorded on OA8338 (2nd quarter of the 18th c.) and OA8318 (mid 17th c.) enamelled watches (see Supplementary Material for details).

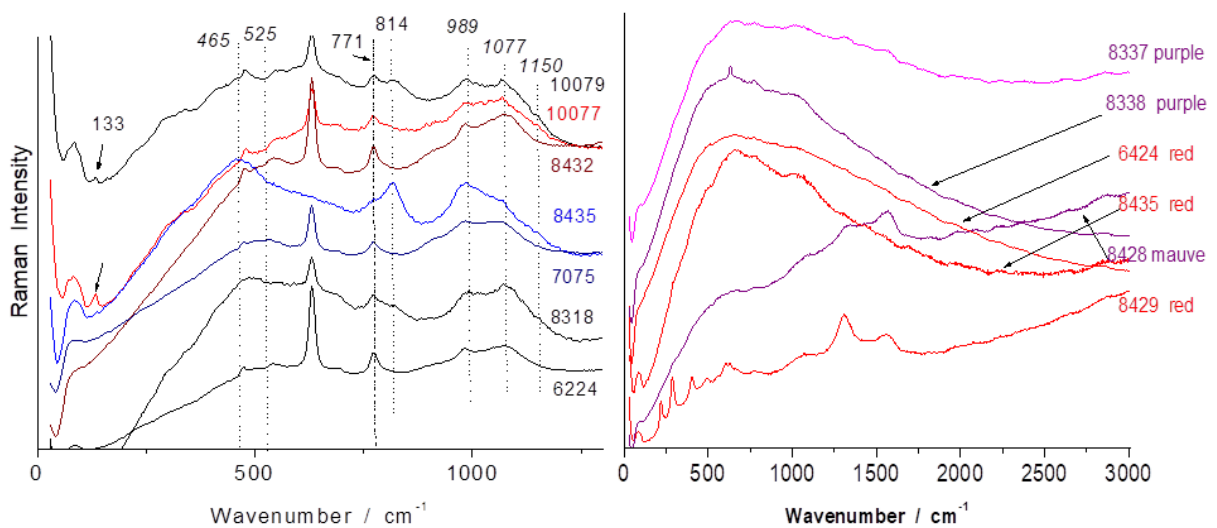


Fig. 7: Comparison of Raman spectra recorded on blue (left) and red-to-purple (right) areas.

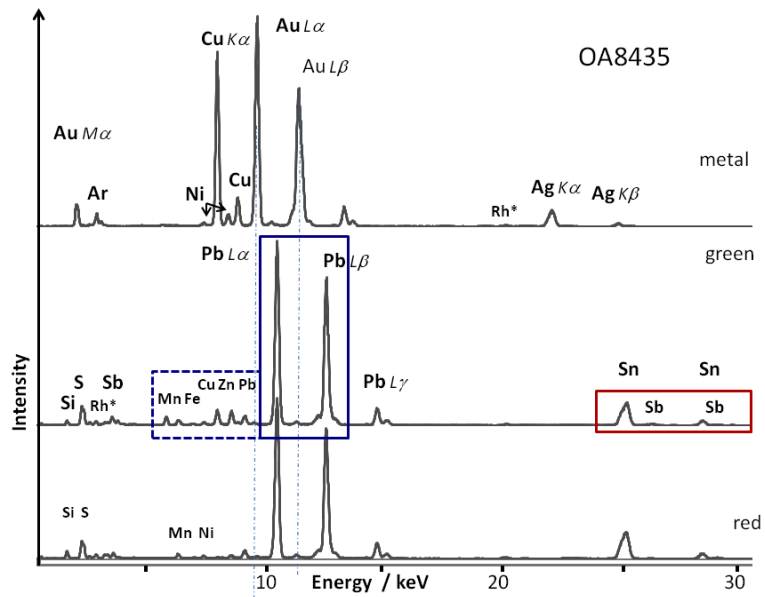


Fig. 8. Representative pXRF spectra recorded on (top) the metal substrate (OA8435), green and red enamels. Details of selected energy windows are shown in Figs 9 and 10.

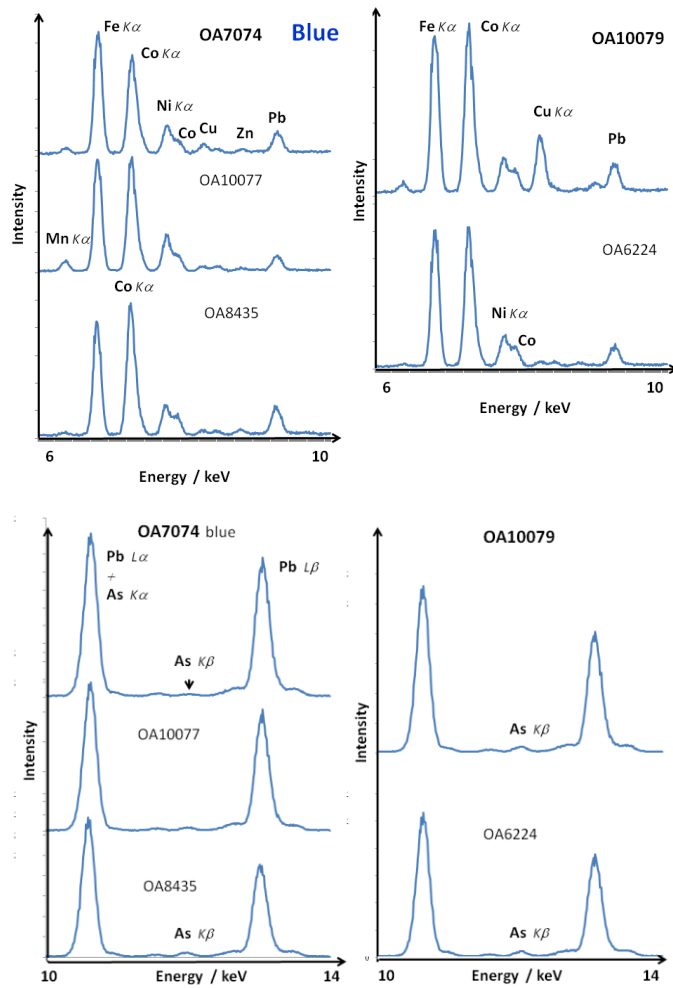


Fig. 9. Representative pXRF spectra recorded in blue areas for energy windows characteristic of the companion elements of cobalt ores.

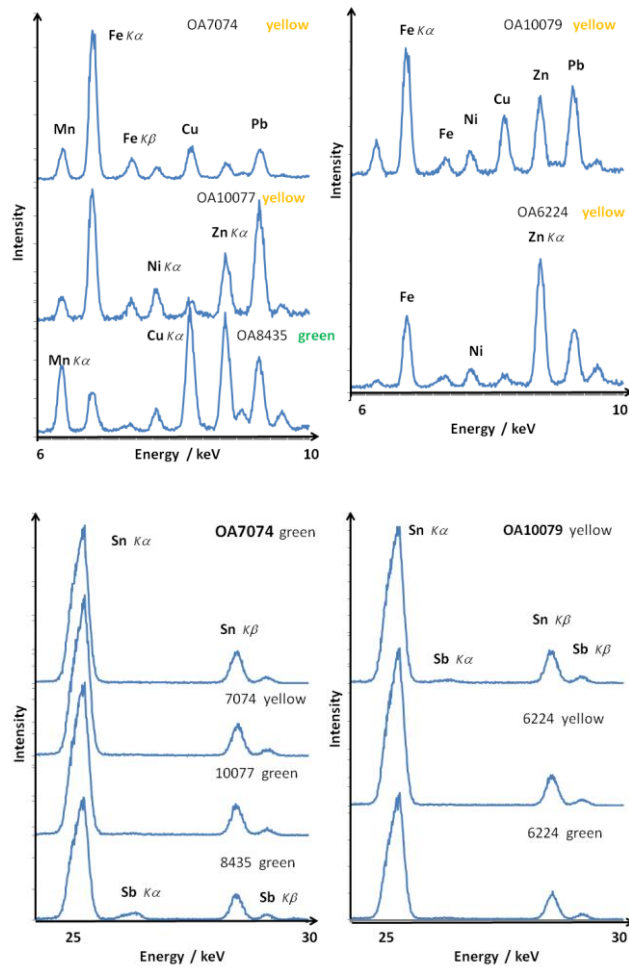


Fig. 10. Representative pXRF spectra recorded in yellow and green areas for energy windows characteristic of elements that could incorporate into the lead pyrochlore solid solution.



Fig. 11. Comparison of the painting technique of the 17th (top) and 18th century (bottom) enamels.